HHS Public Access

Author manuscript

Nat Immunol. Author manuscript; available in PMC 2009 December 01.

Published in final edited form as:

Nat Immunol. 2009 June ; 10(6): 655–664. doi:10.1038/ni.1735.

RAG1 and ATM coordinate monoallelic recombination and nuclear positioning of immunoglobulin loci

Susannah L. Hewitt[1,*], **Bu Yin**[2,*], **Yanhong Ji**[3], **Julie Chaumeil**[1], **Katarzyna Marszalek**[1], **Jeannette Tenthorey**[1], **Giorgia Salvagiotto**[4], **Natalie Steinel**[2], **Laura B. Ramsey**[5], **Jacques Ghysdael**[6], **Michael A. Farrar**[5], **Barry P. Sleckman**[7], **David G. Schatz**[3,9], **Meinrad Busslinger**[4], **Craig H. Bassing**[2,*], and **Jane A. Skok**[1,8,*]

[1]Department of Pathology, New York University School of Medicine, 550 1st Avenue, MSB 531, New York, NY10016, USA

[2]Department of Laboratory Medicine and Pathology, Center for Childhood Cancer Research, Children's Hospital of Philadelphia, University of Pennsylvania School of Medicine, Abramson Family Cancer Research Institute, Philadelphia, PA 19104

[3]Department of Immunobiology Yale University School of Medicine, New Haven, CT 06520.

[4]Research Institute of Molecular Pathology, Vienna Biocenter, Dr. Bohr-Gasse 7, A-1030 Vienna, Austria

[5]Dept. Of Laboratory Medicine and Pathology, University of Minnesota, Minneapolis, MN 55455

[6]Institut Curie, CNRS UMR146, Centre Universitaire, Orsay, France

[7]Department of Pathology and Immunology, Washington University School of Medicine, St. Louis, MO 63110.

[8]The Department of Immunology and Molecular Pathology, Division of Infection and Immunity, University College London, London W1T 4JF, United Kingdom.

[9]Howard Hughes Medical Institute, Yale University School of Medicine, New Haven, CT 06520.

Abstract

Coordinated recombination of homologous antigen receptor loci is thought to be important for allelic exclusion. Here, we show that homologous *Ig* alleles pair in a stage-specific manner that mirrors the recombination patterns of these loci. The frequency of homologous *Ig* pairing was substantially reduced in the absence of the RAG1-RAG2 recombinase and was rescued in *Rag1*$^{-/-}$ developing B cells with a transgene expressing a RAG1 active site mutant that supports DNA binding but not cleavage. The introduction of DNA breaks on one *Ig* allele induced ATM-dependent repositioning of the other allele to pericentromeric heterochromatin. ATM activated by

Correspondence should be addressed to J.A.S. (jane.skok@med.nyu.edu) Jane A. Skok **Tel: 212 263 0504**.

*Joint first or last authors

Competing Interests Statement The authors declare that they have no competing financial interests.

the cleaved allele acts *in trans* on the uncleaved allele to prevent bi-allelic recombination and chromosome breaks or translocations.

Keywords

Igh; *Igk*; homologous pairing; recombinase enzyme; ATM; pericentromeric recruitment; allelic exclusion and V(D)J recombination

INTRODUCTION

Immunoglobulin (*Ig*) and T cell receptor (*Tcr*) loci are assembled through the rearrangement of variable (V), diversity (D), and joining (J) gene segments. V(D)J recombination involves synapsis of compatible conserved recombination signal sequences (RSSs) that flank the V, D and J gene segments of these genes1-3. The lymphocyte-specific V(D)J recombinase enzyme consisting of RAG1 [http://www.signaling-gateway.org/molecule/query?afcsid=A002009] and RAG2 [http://www.signaling-gateway.org/molecule/query?afcsid=A002010] mediates synapse formation and introduces DNA double-strand breaks (DSBs) between the two participating gene segments and their flanking RSSs. The RAG recombinase (unless specifically referring to the individual proteins the recombinase will hereafter be referred to as RAG) additionally stabilize recombination intermediates by holding the broken DNA ends in place and shuttling them into the non-homologous end-joining (NHEJ) DSB repair pathway4,5. In addition, the Ataxia Telangiectasia mutated (ATM) [http://www.signaling-gateway.org/molecule/query?afcsid=A000349] repair-checkpoint protein stabilizes post-synaptic cleavage complexes and coordinates DSB repair with the G1-S cell cycle checkpoint to suppress chromosomal translocations and lymphomas that arise from aberrant V(D)J recombination events6-10.

Ig recombination takes place during B cell development in the bone marrow with each developmental stage delineated by distinct recombination events. Temporally ordered rearrangement of the immunoglobulin heavy chain (*Igh)* locus initiates with D_H-to-J_H recombination in pre-pro-B cells prior to commencement of V_H-to-DJ_H rearrangement in pro-B cells. At the pro-B cell stage of development, up-regulation of the B cell specific transcription factor, Pax5, induces locus contraction on both alleles11-14 enabling V_H-to-DJ_H rearrangement of mid and distal V_H gene families. The mechanisms that coordinate the individual *Ig* recombination steps have not been elucidated. Based upon the rearrangement status of *Igh* alleles in Abelson-murine leukemia virus-transformed developing B cells and mature B cell hybridomas15 it has been postulated that both *Igh* alleles undergo concurrent D_H-to-J_H rearrangement within a single cell and then one allele undergoes V_H-to-DJ_H rearrangement. However, to date there are few studies that have investigated the targeting of individual *Igh* alleles during V(D)J recombination in primary cells and, thus, no direct evidence to support simultaneous biallelic D_H-to-J_H rearrangement.

Allelic exclusion is initiated, established and maintained during B cell development and enforces clonality and monospecific recognition by the B cell receptor expressed on individual B lymphocytes. Allelic exclusion of the *Igh* locus is initiated at the pro-B cell stage of development as only one allele undergoes functional rearrangement. This implies a

mechanism for ensuring that both alleles do not undergo simultaneous V_H-to-DJ_H recombination, but to date none has been identified. Establishment of allelic exclusion at the pro-B to pre-B cell transition inhibits V_H-to-DJ_H recombination of the second DJH-rearranged allele during *Igk* light chain rearrangement. In pre-B cells, rearrangement at the *Igk* locus is preceded by biallelic locus contraction and, in contrast to the *Igh*, one *Igk* allele is positioned at pericentromeric heterochromatin prior to the onset of rearrangement13,16. This process is thought to contribute to allelic exclusion by reducing accessibility to one allele during recombination17. It is not known what mechanism regulates the differential treatment of *Igk* alleles.

We have investigated potential mechanisms by which V(D)J recombination is coordinated on the two alleles of the *Igh* and *Igk* loci during B cell development. Here we show that the V(D)J recombinase and the cellular DNA damage response machinery coordinate DNA cleavage and nuclear positioning of *Ig* loci to initiate allelic exclusion and preserve genomic integrity during antigen receptor rearrangement.

RESULTS

Homologous pairing of *Igh* and *Igk* alleles

It is known that pairing of X chromosomes has an important role in X inactivation during early development of female mammals18-20. To determine whether ‘pairing’ might have a role in regulating *Ig* loci, we analyzed the frequency of paired homologous *Ig* alleles in sorted bone marrow primary B lymphocytes of different developmental stages (Supplementary Fig. 1 online) and in mouse embryonic fibroblasts (MEFs). For these experiments, we performed two-color three-dimensional (3-D) DNA fluorescent *in situ* hybridization (FISH) experiments and subsequent confocal microscopy analysis as described previously13 (Fig. 1a—d and Supplementary Tables 1,2 online). The *Igh* DNA BAC probes used, CT7-526A21 and CT7-34H6, map to the distal V_H gene region located at the 5′ end of the *Igh* locus and the 3′ constant (C_H) region, respectively (Fig. 1b). The *Igk* BAC DNA probes used, RP23-101G13 and RP24-387E13, map to the distal $V_κ24$ gene region located at the 5′ end of the *Igk* locus and the 3′ constant ($C_κ$) region, respectively (Fig. 1d). Homologous pairing of *Ig* alleles was scored if at least one end of the homologous *Igh* and *Igk* alleles were separated by less than 1 μm. At the *Igh* locus we observed homologous pairing of the two alleles in 24% of $CD19^-$ pre-pro-B cells and in 21% of $CD19^+$ pro-B cells. (Fig. 1a,b and Supplementary Table 1). Similarly at the *Igk* locus we observed interallelic pairing in 18–20% of pre-B cells, early immature B cells and late immature B cells (Fig. 1c,d and Supplementary Table 2). Pairing of homologous *Igh* and *Igk* alleles was seen in 8–10% of B cells of developmental stages where recombination does not occur but where the locus is being transcribed. This result is significantly different to the low frequency of interallelic pairing (2%) we observed for both *Igh* and *Igk* in MEFs where the loci are transcriptionally inactive (Fig. 1a,b,c and Supplementary Table 1,2). These data indicate that pairing of homologous *Igh* and *Igk* alleles occurs in a lineage and developmental stage specific manner that mirrors recombination of these loci

Antigen receptor locus rearrangement correlates with germline transcription, open chromatin, and contraction of *Ig* and *Tcr* loci12,13,21,22. In the absence of Pax5, V_H

germline transcription, histone acetylation of V_H chromatin and expression of *Rag1* and *Rag2* are normal, but both *Igh* contraction and V_H-to-DJ_H rearrangement of mid and distal V_H genes are substantially impaired11,23,24. To determine whether *Ig* pairing might be influenced by locus conformation, we analyzed the frequency of pairing of homologous *Igh* alleles in short-term cultured wild-type and *Pax5*$^{-/-}$ pro-B cells. Homologous pairing was substantially reduced in *Pax5*$^{-/-}$ pro-B cells (Fig. 1e,f and Supplementary Table 3 online). These data indicate that homologous *Igh* pairing occurs when the locus is present in distinct conformations at two phases of B cell development during D_H-J_H and V_H-DJ_H recombination. Pairing of different *Igh* regions or pairing of the same region mediated by different factors could provide a mechanism to prevent the initiation of V_H-DJ_H rearrangement prior to completion of D_H-J_H rearrangement on both alleles.

RAG1 mediates homologous pairing of *Ig* alleles

The identical developmental stage specific patterns of *Ig* pairing and rearrangement suggests that there may be a mechanistic link between these two phenomena. To test this we next asked whether the V(D)J recombinase contributes to interallelic pairing of *Igh* and *Igk* alleles. For this we analyzed the frequency of pairing of homologous *Ig* alleles in primary bone marrow derived B lymphocytes of different developmental stages sorted from wild-type, *Rag1*$^{-/-}$ or *Rag1*$^{-/-}$ mice expressing a functionally rearranged B1.8 *Igh* knock-in25 and/or *Rag1*^{D708A} transgene26. Expression of the B1.8 rearranged *Igh* knock-in drives B cell development to the pre-B cell stage25 enabling analysis of the *Igk* locus in *Rag1*$^{-/-}$ mice. The D708A active site mutation of the RAG1 protein prevents DNA cleavage but still enables binding and synapsis of RSSs by the RAG complex26-28. A significantly higher percentage of wild-type CD19$^-$ pre-pro-B cells (24%) and CD19$^+$ pro-B cells (22%) contained paired *Igh* alleles as compared to *Rag1*$^{-/-}$ CD19$^-$ pre-pro-B cells (12%) or CD19$^+$ pro-B cells (12%) (Fig. 2a). Likewise, *Igk* allele pairing was significantly higher in B1.8 pre-B cells (18%) compared to *Rag1*$^{-/-}$ B1.8 pre-B cells (9%) (Fig. 2b). Notably, the frequencies at which *Igh* and *Igk* alleles were paired in *Rag1*$^{-/-}$ *Rag1*^{D708A} CD19$^+$ pro-B cells (28%) and *Rag1*$^{-/-}$ *Rag1*^{D708A} B1.8 pre-B cells (17%), respectively, were increased (*Igh*) or comparable (*Igk*) to those observed in wild-type pro-B cells or B1.8 pre-B cells, respectively. Collectively, these data demonstrate that high frequencies of interallelic *Ig* pairing are dependent upon RAG1 expression, but not on RAG DNA cleavage activity.

RAG1 differentially marks paired *Ig* alleles

X inactivation takes place in developing female (XX) cells and seems to be dependent on pairing of X-inactivation centers present on the two individual X chromosomes18-20. To determine whether the two processes share a common function we next asked whether *Ig* loci pairing occurs prior to the initiation of V(D)J recombination on one allele and, if so, whether this pairing might silence or reduce the accessibility of the unrearranged *Ig* allele upon separation of paired *Ig* alleles. We first analyzed by confocal microscopy the position of paired *Igh* alleles relative to pericentromeric heterochromatin by performing three-color 3-D DNA FISH using the two BACs CT7-526A21 and CT7-34H6 in combination with a γ-satellite probe, which hybridizes to major satellite centromeric repeats. Wild-type pre-pro-B and pro-B cells had paired *Igh* alleles that were predominantly positioned close to pericentromeric heterochromatin with one allele juxtaposed to this repressive compartment

and the other allele located in a euchromatic region of the nucleus (Fig. 3a,b and Supplementary Table 4 online). These data indicate that homologously paired *Igh* alleles are differentially marked as defined by their nuclear locations.

To determine whether recombination could be a prerequisite for differential marking, we next analyzed the position of paired *Igh* alleles relative to pericentromeric heterochromatin in sorted *Rag1*$^{-/-}$ pre-pro-B and pro-B cells in the presence or absence of the *Rag1*^{D708A} transgene (Fig. 3a,b and Supplementary Table 4). We observed that paired *Igh* alleles in *Rag1*$^{-/-}$ pre-pro-B and pro-B cells had one *Igh* allele associated with pericentromeric heterochromatin at a significantly lower frequency (19% and 9%, respectively) than in comparable wild-type populations (45% and 39%, respectively). This difference could not be rescued by the presence of the *Rag1*^{D708A} transgene. Hence, differential nuclear positioning of *Igh* alleles is induced by RAG-mediated cleavage. Recombination also affected the relative distribution of *Igh* in total pre-pro-B and pro-B populations (Fig. 3c and Supplementary Table 5 online) indicating that RAG-mediated DNA cleavage was required for monoallelic *Igh* association with pericentromeric heterochromatin in cells where alleles were paired or unpaired.

We next analyzed the V_H-to-DJ_H rearrangement status of *Igh* alleles relative to pericentromeric heterochromatin by performing three-color 3-D DNA FISH using a γ-satellite probe in combination with the C_H BAC and a BAC probe, RP24-275L15, which hybridizes to the intergenic region between the V_H and D_H gene segments (Fig. 3d). Any V_H-to-DJ_H recombination event will result in deletion of this intergenic region and loss of this signal. We analyzed cells containing one germline (275L15$^+$) and one V_HDJ_H rearranged (275L15$^-$) *Igh* allele and observed the germline (275L15$^+$) *Igh* allele associated with pericentromeric heterochromatin in 67% of pro-B cells with unpaired *Igh* alleles and in 81% of pro-B cells with paired *Igh* alleles (Fig. 3e and Supplementary Table 6 online). We additionally looked at the position of paired unrearranged *Igh* alleles in cells in which both 275L15 signals were present (Fig. 3f and Supplementary Table 4). Our results indicate that 78% of unrearranged paired alleles were positioned in euchromatic regions of the cell. Taken together our data suggest that unrearranged alleles pair up in a recombinase-dependent manner in euchromatic regions of the nucleus. Differential marking of paired alleles, following RAG1-mediated cleavage, directs the unrecombined allele to pericentromeric heterochromatin while the rearranged allele remains in a euchromatic region of the nucleus.

We next analyzed the position of *Igk* alleles relative to pericentromeric heterochromatin by performing DNA FISH using the $V_κ$ and $C_κ$ BACs in combination with a γ-satellite probe. We compared the nuclear location of paired *Igk* alleles in control B1.8 pre-B cells with paired *Igk* alleles in *Rag1*$^{-/-}$ B1.8 and *Rag1*$^{-/-}$ *Rag1*^{D708A} B1.8 pre-B cells. Substantially less pericentromeric association of paired *Igk* occurred in *Rag1*$^{-/-}$ cells (27%) compared to 80% of the control cells (Fig. 3g,h and Supplementary Table 7 online), and, in contrast to *Igh*, expression of the *Rag1*^{D708A} mutant rescued this effect (78%). Furthermore RAG1 expression, independent of RAG-mediated DNA cleavage, was required for monoallelic *Igk* association with pericentromeric heterochromatin in overall pre-B populations (Fig. 3i and Supplementary Table 8 online).

ATM directs allelic repositioning

We have recently demonstrated that RAG-mediated *Ig* cleavage activates a multi-functional genetic program that is, in part, dependent upon the ATM repair-checkpoint protein29. We next analyzed the relative positions of *Igh* loci in pre-pro-B and pro-B cells from *Atm*$^{-/-}$ mice to determine whether ATM dependent signals were required for RAG-cleavage induced association of unrearranged *Igh* alleles with pericentromeric heterochromatin. Although we observed that homologous pairing of *Igh* alleles occurs at the same high frequency in *Atm*$^{-/-}$ and wild-type pre-pro-B and pro-B cells, paired *Igh* alleles remain predominantly euchromatic (72% and 75%, respectively) in contrast to what was observed in the equivalent wild-type populations (44% and 41%, respectively; Fig. 4a,b and Supplementary Table 4). In addition the overall frequency of mono- and biallelic pericentromeric recruitment of *Igh* alleles was reduced in *Atm*$^{-/-}$ pre-pro-B and pro-B cells compared to that seen in the equivalent wild-type populations (41% and 34%, respectively; Fig. 4c, d and Supplementary Table 5).

At the *Igk* locus, again comparable frequencies of homologous pairing occurred in *Atm*$^{-/-}$ and wild-type pre-B cells (Fig. 4e and Supplementary Table 2) but differential marking of paired *Igk* alleles was reduced (50% in *Atm*$^{-/-}$ pre-B cells compared to 68% in wild-type pre-B cells) and we additionally observed significantly reduced monoallelic pericentromeric recruitment of *Igk* in the overall population of *Atm*$^{-/-}$ pre-B cells (39% in *Atm*$^{-/-}$ pre-B cells compared to 71% in wild-type pre-B cells) (Fig. 4d,f,g and Supplementary Tables 7,8). Collectively our data suggest that the activation of ATM by RAG-mediated cleavage during *Ig* rearrangement provides signals by which the unrearranged allele is associated with pericentromeric heterochromatin.

ATM prevents biallelic RAG-mediated cleavage

ATM rapidly phosphorylates the H2AX histone variant to form γ-H2AX in chromatin around DSBs, including those induced by RAG during *Tcra* rearrangements in thymocytes8. To determine whether initiation of V(D)J recombination is coordinated between homologous *Ig* alleles, we investigated whether RAG-dependent H2AX phosphorylation along *Ig* loci occurred in a monoallelic or biallelic manner in developing B cells. Importantly, the localization of γ-H2AX with *Igh* was absolutely dependent on recombinase enzymes since these foci are never associated with *Igh* loci in *Rag1*$^{-/-}$ cells (Supplementary Fig. 3 online). In cells containing γ-H2AX-associated *Igh* signals, 97.2% of pre-pro-B and 99.2% of pro-B cells had monoallelic γ-H2AX association with *Igh* whereas 2.8% of pre-pro-B and 0.8% of pro-B cells had biallelic association. Similarly in pre-B cells containing *Igk* alleles coincident with γ-H2AX 94.8% had monoallelic association with *Igk* while 5.2% were biallelically associated (Supplementary Fig. 4a,b online and Supplementary Tables 9, 10 online). Localization of γ-H2AX foci on both alleles of *Igh* or *Igk* could represent either simultaneous biallelic RAG-generated DSBs or a lag in the resolution of γ-H2AX foci after repair of monoallelic DSBs. Regardless, these data indicate that RAG-mediated cleavage occurred on only one allele at a time in the majority of primary bone marrow cells during D_H-to-J_H, V_H-to-DJ_H and V_κ-to-J_κ recombination.

Monoallelic targeting of the V(D)J recombinase could reflect either an inefficient or regulated process. To distinguish between these possibilities, we calculated the number of cells in which we would expect to find biallelic association of γ-H2AX (as judged by the presence of γ-H2AX foci) if recombinase targeting were not regulated and compared it with the actual number observed. If γ-H2AX foci are observed in x% of a given population, the expected frequency of biallelic recombination would be x% of x%. Notably, the percentage of cells in which we actually observed biallelic association of γ-H2AX with *Igh* and *Igk* in cells undergoing recombination was significantly lower than the predicted frequency (Fig. 5a—e and Supplementary Table 9, 10). These observations support the notion that D_H-to-J_H, V_H-to-DJ_H and V_κ-to-J_κ rearrangement each occur on one allele at a time and that monoallelic V(D)J recombination occurs as a result of regulated or restricted targeting of RAG-mediated cleavage and is not simply a result of inefficient recombination.

Since activation of ATM by RAG-mediated cleavage provides signals by which the unrearranged allele associated with pericentromeric heterochromatin, we next asked whether ATM restricted RAG-mediated cleavage to one allele at a time. For this we carried out γ-H2AX-*Ig* immuno-DNA FISH on developing B lymphocytes sorted from the bone marrow of *Atm*$^{-/-}$ mice. Compared to the equivalent wild-type cells, the average number of γ-H2AX foci was reduced but not absent in *Atm*$^{-/-}$ pro-B cells (5.97 compared to 5.65, respectively) and pre-B cells compared (5.05 and 3.18, respectively) indicating that many γ-H2AX foci in developing B cells were generated by another H2AX kinase such as DNA-PKcs or ATR30. In *Atm*$^{-/-}$ cells containing *Igh* alleles coincident with γ-H2AX, 10.3% of pre-pro-B and 3.1% of pro-B cells had biallelic association and in pre-B cells containing *Igk* alleles coincident with γ-H2AX 18.8% had biallelic association with *Igk* (Fig. 5d,e and Supplementary Fig. 4a,b and Supplementary Table 9,10). We next calculated the predicted frequency at which we would expect to see biallelic DSBs introduced on *Igh* and *Igk* in cells where these loci are undergoing rearrangement and compared these values to the actual frequency at which we observed biallelic localization of γ-H2AX on *Ig* loci in these cells. No significant differences were found between predicted frequencies for biallelic localization of γ-H2AX on *Igh* and *Igk* in pre-pro-B cells and pre-B cells, respectively, and the frequencies that we actually observed (Fig. 5a,c). Although the introduction of DSBs on both alleles was also elevated in *Atm*$^{-/-}$ pro-B cells, the increase was less marked than what we observed in *Atm*$^{-/-}$ pre-pro-B cells. However, as has been previously reported by others31, we observed broken and/or missing *Igh* alleles in a significant percentage of *Atm*$^{-/-}$ pro-B cells. In this context, deregulated targeting of the recombinase machinery during D_H-to-J_H rearrangement in *Atm*$^{-/-}$ pre-pro-B cells could interfere with V_H-to-DJ_H recombination at the later pro-B cell stage because of a reduced number of intact *Igh* loci. Collectively, our observations suggest that ATM-mediated repositioning of unrearranged *Ig* alleles with pericentromeric heterochromatin reduced accessibility and inhibited biallelic RAG-mediated cleavage.

ATM prevents biallelic *Igk* chromosome breaks

Treatment of NHEJ-deficient v-Abl transformed (Abl) pre-B cell lines with the Abl kinase inhibitor STI571 leads to G1 arrest, *Rag1* and *Rag2* expression and accumulation of unrepaired RAG-generated *Igk* coding ends (CEs), which activate ATM-dependent signals29,32. To directly evaluate whether ATM prevents biallelic RAG-mediated cleavage,

we treated *Rag2*$^{-/-}$, *Artemis*$^{-/-}$ and *Artemis*$^{-/-}$*Atm*$^{-/-}$ cells with STI571 for 1–7 days and performed J_κ locus Southern blot analysis on DNA isolated from these cells. Artemis is an NHEJ factor required for opening CEs so that RAG-generated DSBs are repaired33,34. Retention of the germline J_κ band was observed in the control *Rag2*$^{-/-}$ cells (Fig. 6a, while in *Artemis*$^{-/-}$ cells, we found a 30–50% reduction in the germline J_κ band and a corresponding increase in J_κ CE bands (Fig. 6a and Supplementary Fig. 5 online). These data demonstrate that RAG-mediated cleavage occurred on half of the *Igk* alleles within these cells. In contrast, we found an 80% reduction in the germline J_κ band and a corresponding increase in J_κ CE bands in *Artemis*$^{-/-}$*Atm*$^{-/-}$ cells (Fig. 6a and Supplementary Fig. 5), indicating that RAG-mediated cleavage occurred on more than half of the *Igk* alleles within these cells. Similar findings were observed in independently derived cell lines (Supplementary Fig. 5). These data suggest that J_κ CEs activate ATM signals that prevent RAG-mediated cleavage of the other *Igk* loci until NHEJ-mediated formation of $V_\kappa J_\kappa$ coding joints.

During V(D)J recombination, ATM maintains CEs within repair complexes and prevents RAG-initiated genomic instability31,32. To investigate whether ATM prevents biallelic dissociation of*Igk* CEs and biallelic chromosome breaks or translocations involving *Igk* we performed two-color DNA FISH using a 5′ V_κ BAC RP24-243E11 and a 3′ C_κ BAC RP23-341D5 probe on G1 nuclei prepared from STI57-treated *Artemis*$^{-/-}$*p53*$^{-/-}$ and *Artemis*$^{-/-}$*Atm*$^{-/-}$ pre-B cells. We used *Artemis*$^{-/-}$*p53*$^{-/-}$ cells rather than *Artemis*$^{-/-}$ cells so that the ATM-p53-dependent G1-S checkpoint was impaired as in *Artemis*$^{-/-}$*Atm*$^{-/-}$ cells. We observed coincident (<1 μm) probe signals on both alleles in 85% of *Artemis*$^{-/-}$*p53*$^{-/-}$ nuclei, with non-coincident probe signals on one allele in 15% and both alleles in less than 1% of nuclei (Fig. 6b). We found coincident probe signals on both alleles in 50% of *Artemis*$^{-/-}$*Atm*$^{-/-}$ nuclei, with non-coincident probe signals on one allele in 41% and on both alleles in 10% of nuclei (Fig. 6b). The difference between non-coincident signals in 1% of *Artemis*$^{-/-}$*p53*$^{-/-}$ nuclei and 10% of *Artemis*$^{-/-}$*Atm*$^{-/-}$ nuclei was statistically significant (P = 0.005). Next, we performed FISH using the V_κ and C_κ BACs and a chromosome 6 ‘paint’ on metaphase spreads prepared from untreated cells or cells that had been released back into cycle by removing STI571. We observed chromosome 6 translocations in less than 3% of metaphases prepared from untreated cells (data not shown). We found RAG-induced *Igk* chromosome breaks or translocations in 4% of *Artemis*$^{-/-}$ *p53*$^{-/-}$ cells, whereby lesions arose from a single *Igk* allele (Fig. 6c). In contrast, we observed *Igk* chromosome breaks or translocations in 66% of *Artemis*$^{-/-}$*Atm*$^{-/-}$ cells, with 30% of cells containing lesions arising from both *Igk* alleles (Fig. 6c). The difference between the absence of biallelic *Igk* abnormalities in *Artemis*$^{-/-}$*p53*$^{-/-}$ nuclei and 30% of *Artemis*$^{-/-}$*Atm*$^{-/-}$ nuclei was statistically significant (P = 0.005). Collectively, these data demonstrate that ATM regulates monoallelic RAG-mediated cleavage of homologous *Igk* loci to prevent biallelic V(D)J recombination errors.

Igh pairing can occur beyond the pro-B cell stage

A prediction of our findings is that in *Atm*$^{-/-}$ mice allelic exclusion could be violated. However flow cytometry analyses for surface and cytoplasmic IgH expression of *Atm*$^{-/-}$ mice containing allotypically marked *Igh* alleles indicate that *Igh* allelic exclusion was maintained (Fig. 7a and Supplementary Fig. 6 online). We next asked whether maintaining

accessibility of the *Igh* locus at the pre-B cell stage could maintain a high frequency of homologous association leading to silencing of one allele in cells that are expressing two functionally rearranged *Igh* alleles. Interleukin 7 receptor (IL-7R) signaling mediated by the transcription factor STAT5 is thought to be responsible for histone acetylation and transcription of distal V_H genes at the pro-B cell stage35. Following functional rearrangement of one *Igh* allele, pre-BCR signaling results in attenuation of IL-7R signaling, which leads to histone deacetylation and reduced V_H gene accessibility36. The expression of a constitutively active *Stat5A* (*caStat5*) transgene37 may therefore prevent the loss of *Igh* accessibility at the pre-B cell stage. To determine this, we used mice that expressed either *caStat5A* or *caStat5B* transgenes37,38. The results of the experiments with the two transgenic mice strains were equivalent, and data are shown for B cells derived from the *caStat5B* mice. We performed DNA FISH with sorted developing B cells from *caStat5* and wild-type mice as described in Fig. 4. In contrast to wild-type pre-B cells, recruitment of one *Igh* allele to pericentromeric clusters did not occur in *caStat5* pre-B cells and was delayed until the immature B cell stage (Fig. 7b and Supplementary Table 5). These data indicate that inactivation of STAT5 was pivotal in changing accessibility at the *Igh* locus as defined here by nuclear location and that STAT5 was important in translating signals from the pre-BCR into alterations of *Igh* position within the nucleus. To determine whether accessibility could influence homologous *Igh* pairing beyond the pro-B cell stage, we examined the frequency of association of the two *Igh* alleles in pre-B and immature B cells from wild-type and *caStat5* mice. In contrast to wild-type cells, the association of *Igh* alleles remained high in *caStat5* pre-B cells and started to decline only at the subsequent immature B cell stage (Fig. 7c,d and Supplementary Table 1), when one *Igh* allele also became repositioned to pericentromeric heterochromatin (Fig. 7b and Supplementary Table 5). In summary, the frequency of *Igh* pairing depended on accessibility and was reduced when one *Igh* allele repositioned to a repressive nuclear compartment in pre-B cells.

Association of *Igh* with the *Igk* locus occurs at the pre-B cell stage. Analysis of sorted wild-type and *caStat5* B lymphocytes at different developmental stages revealed that the frequency of association of *Igh* and *Igk* alleles was substantially reduced in pre-B and early immature B cells of *caStat5* mice compared to wild-type mice (Supplementary Fig. 7a online and Supplementary Table 11 online). As association of the *Igh* locus with an *Igk* allele is a prerequisite for decontraction of the *Igh* locus in pre-B cells39 we analyzed the contraction state of the *Igh* locus by 3-D FISH in developing B lymphocytes of *caStat5* mice. Consistent with the low frequency of association between *Igh* and *Igk* alleles, the *Igh* locus remained contracted in pre-B and immature B cells of *caStat5* mice (Supplementary Fig. 7b and Supplementary Table 3). We have previously shown that ongoing accessibility of the *Igh* locus in 3′ *Igk* enhancer-deficient mice ($3'E_\kappa^{-/-}$) pre-B cells results in an increase of rearrangements involving distal V_HJ558 gene segments as judged by an absence of CT7-526A21 FISH signals, which detects more proximally located V_HJ558 gene segments39. A similar FISH analysis of *caStat5* pre-B cells revealed that these CT7-526A21 VHJ558 gene segments were also deleted more frequently as compared with wild-type pre-B cells (Fig. 7e,f and Supplementary Table 12 online). Ongoing V_H-DJ_H recombination was confirmed by ligation-mediated PCR (LM-PCR) to assay for the presence of recombinase mediated DSBs at *Igh* locus RSSs. DNA breaks represent reaction intermediates of

rearrangement (Supplementary Fig. 7c). Flow cytometric analysis of mice heterozygous for two allotypically marked *Igh* alleles indicated, however, that allelic exclusion was not violated in splenic B cells of *caStat5* mice (Supplementary Fig 8 online) similar to $3'E_\kappa^{-/-}$ mice39,40.

In $Atm^{-/-}$ mice accessibility of the *Igh* locus was prolonged beyond the pro-B cell stage as it was in the $3'E_\kappa^{-/-}$ and *caStat5* mice. In all three genotypes ongoing accessibility of *Igh* alleles at the pre-B cell stage in $Atm^{-/-}$ mice was correlated with a high frequency of association of *Igh* alleles (Fig. 7c,g,h and Supplementary Table 1 (data for the $3'E_\kappa^{-/-}$ mice is not shown)). Furthermore in all the genotypes we have examined allelic exclusion remained intact despite ongoing accessibility leading to increased V_HJ558 gene rearrangement or biallelic RAG-mediated cleavage. These data support the idea that there is a second checkpoint for establishing allelic exclusion at the pre-B to immature B transition41, which could be mediated by homologous pairing and differential marking of *Igh* alleles in pre-B cells.

DISCUSSION

Generation of a monospecific BCR on individual B cells is thought to be important for preventing autoimmunity but the mechanisms by which this is achieved remain unclear. Based upon our collective observations, we propose a model in which homologous *Igh* and *Igk* alleles proceed through cycles of pairing and separation with V(D)J recombination initiating on a single paired *Ig* allele. RAG-mediated cleavage activates ATM to mediate differential marking of the two alleles, which in turn leads to preferential association of the non-cleaved allele with pericentromeric heterochromatin. We propose that the ATM driven repositioning of the undamaged allele to these repressive nuclear regions enables a mechanism for transiently inhibiting accessibility to the recombinase and provides a time-window in which the RAG-cleaved allele can be repaired, transcribed, translated and tested for functionality. Assembly and expression of a productive V_HDJ_H or $V_\kappa J_\kappa$ rearrangement on the first allele leads to expression of the pre-BCR or BCR and initiation of classical feedback inhibition of further V_H or V_κ rearrangement. The ATM driven marking of the uncleaved allele could be reversed either because DSB repair leads to cessation of ATM-dependent signals, and/or by restoring accessibility. As the accessibility of *Ig* loci is maintained at their respective stage of V(D)J recombination, it is conceivable that changes induced by differential marking of the unrearranged allele could be reversed. This would result in disassociation of the unrearranged allele from pericentromeric heterochromatin and enable another round of pairing, cleavage and repositioning to occur. Such cycles could occur until either a functional V_H-to-DJ_H or V_κ-J_κ rearranged allele is produced or all possible V(D)J recombination events are exhausted and the cell dies. Although we hypothesize that V(D)J recombination initiates on paired *Ig* alleles our data cannot rule out the possibility that RAG-mediated cleavage also occurs on unpaired alleles. However if ATM that is localized on the rearranging allele acts *in trans* to inhibit recombination of the other allele this is more likely to occur if the two *Ig* alleles are closely paired than for the pool of activated ATM to diffuse over a large distance if the two alleles are separated.

In addition to allelic exclusion of antigen receptor loci, monoallelic expression of maternal or paternal genes in mammalian cells includes X-inactivated and autosomal genes. It is known that pairing of X chromosomes has an important role in X inactivation, but the mechanisms leading to monoallelic expression of autosomal genes remain poorly understood. Transient pairing of the two X chromosomes in developing female cells requires transcription of both alleles and ensures that only one chromosome is chosen and targeted for silencing prior to differential epigenetic marking and separation of the homologous alleles18,19. Our data suggest that in parallel with X inactivation, homologous pairing of *Ig* loci contributes to allelic exclusion by ensuring that only one allele is targeted for recombination at any time. Interallelic pairing could therefore be a general mechanism for establishing monoallelic gene expression.

From the ‘selfish gene’ perspective, selective pressure may have forced the adaptive immune system to evolve in higher organisms to ensure the propagation of genetic material from generation to generation. In this context, it has been proposed that antigen receptor allelic exclusion evolved under selective pressure to prevent autoimmunity by ensuring proper positive or negative selection and receptor editing. Here, we propose that allelic exclusion may additionally have evolved from necessity to preserve cellular survival, maintain genomic integrity, and suppress oncogenic translocations during antigen receptor gene rearrangements.

Methods

Mice

The following mice were maintained on the C57BL/6 background and genotyped as described: *Rag1*$^{-/-}$[42] and *Rag2*$^{-/-}$[43]. The mouse *Rag1*-D708A BAC transgene was derived from the HG BAC (≈170 kb), kindly provided by M. Nussenzweig, which spans the *Rag* locus and encodes GFP instead of *Rag2*44. The GAT codon for *Rag1* aspartate 708 was changed to GCG (encoding alanine) by homologous recombination in bacteria. Mice containing the full-length *Rag1*-D708A BAC transgene (copy number 2-3) were bred with *Rag1*$^{-/-}$ mice on the C57BL/6 background to generate *Rag1*$^{-/-}$ *D708A* mice. B1.8mice contain a functionally rearranged Igμ knock-in25. The *Atm*$^{-/-}$ mice were generated through the interbreeding of 129SvEv *Atm*$^{+/-}$ mice and genotyped as described45. The animal care was approved by NYU SoM Institutional Animal Care and Use Committee (IACUC) Protocol #060509-03, Yale IACUC Protocol# 2006-07610 and Children’s Hospital of Philadephia IACUC Protocol # 2007-9-711.

Flow cytometry sorting and analysis

Bone marrow cells were isolated, non-specific antibody staining was suppressed by pre-incubation of cells with CD16/CD32 Fc-block (clone 2.4G2) and cells were purified by flow cytometry on a MoFlo (Dako). All antibody staining was carried out at 4°C for 20 minutes. For sorting of pre-pro-B, pro-B and pre-B populations, cells were stained with lineage markers and streptavidin PE-Cy5.5, IgM FITC, CD25 PE, B220 PE-Cy7, cKit APC, CD19 APC-Cy7 and sorted as lineage marker negative (Lin^{-}), CD25^{-}, IgM^{-}, B220^{+}, cKit^{+} and then either CD19^{-} or CD19^{+} for pre-pro-B cells and pro-B cells respectively. Pre-B cells were

sorted as Lin$^-$, IgM$^-$, B220$^+$, cKit$^-$ CD25$^+$, and CD19$^+$. Alternatively, pro-B, pre-B, early immature and late immature B cells were stained with CD19 APC-Cy7, cKit APC, CD25 PE, IgM PE-Cy7, IgD FITC and pro-B cells sorted as CD19$^+$, cKit$^+$, CD25$^-$ and IgM$^-$, pre-B cells as cKit$^-$, CD19$^+$, CD25$^+$, IgM^{--}, early immature B cells as CD19$^+$, IgM^{lo}, IgD$^-$ and late immature B cells as CD19$^+$, IgM^{hi}, IgD$^-$. The purity of the sorted cells was verified by reanalysis. Antibodies were from BD Biosciences, except where mentioned: CD19 allophycocyanin-Cy7 (APC-Cy7, clone 1D3), CD117 allophycocyanin (cKit APC, 2B8), CD25 R-phycoerythrin (PE or FITC, PC61), IgM R-phycoerythrin-Cy7 (PE-Cy7 or FITC, R6-60.2), IgD fluorescein isothiocyanate (FITC, 11-26c.2a), B220 PE-Cy7 (RA3-6B2). The following lineage (Lin) marker antibodies were used conjugated to biotin and detected with streptavidin-PE-Cy5.5, in order to eliminate lineage-positive cells (Lin$^+$) by electronic gating: CD3e (145-2C11), CD8a (53-6.7), NK1.1 (PK136), Ly6G and 6C (Gr-1, RB6-8C5), CD11b (Mac-1, M1/70), CD11c (eBioscience, N418), TER-119/Erythroid cells. Purification of resting splenic B cells was carried out as described previously46.

Three-dimensional DNA FISH

Cells sorted by flow cytometry were washed in PBS and then were fixed on poly-L-lysine-coated slides for two-color and three-color three-dimensional DNA-FISH analysis as described11. Probes were directly labeled by nick translation with ChromaTide Alexa Fluor 488-5-dUTP, ChromaTide Alexa Fluor 594-5-dUTP (Molecular Probes) or dUTP-indodicarbocyanine (GE Healthcare). The γ-satellite probe was prepared from a plasmid containing eight copies of the γ-satellite repeat sequence46 and was directly labeled with dUTP—fluorescein isothiocyanate (Roche; Enzo Biochem) or dUTP-indodicarbocyanine.

Immunofluorescence and DNA FISH-immunofluorescence

Detection of γ-H2AX alone was carried out on cells adhered to poly-L lysine coated coverslips, fixed with 2% paraformaldehyde in PBS for 10 min at 22°C and permeabilized for 5 min with 0.4% Triton in PBS. Non-specific antibody binding was blocked with 2.5% BSA, 10% normal goat serum and 0.1% Tween-20 in PBS for 30 min. γ-H2AX staining was carried out using an antibody against phosphorylated serine-139 of H2AX (clone JBW301, Millipore) diluted 1:500 in blocking solution for 1 h at 22°C. Cells were rinsed with 0.2% BSA, 0.1% Tween-20 in PBS and stained with goat-anti-mouse IgG Alexa Fluor 488 or 633 (Invitrogen) for 1 h. Cells were rinsed with 0.1% Tween-20 in PBS and mounted in Vectashield (Vector Laboratories) containing DAPI to counterstain total DNA.

Combined detection of γ-H2AX and *Igh* was carried out on cells fixed and stained for γ-H2AX detection as above. Following the final 0.1% Tween-20 in PBS rinse cells were post fixed in 3% paraformaldehyde for 10 min at 22°C, permeabilized in 0.7% Triton-X-100 in 0.1M HCl for 15 min at 0°C and treated with 0.1 mg/ml RNaseA for 30 min at 37°C. Cells were then denatured with 1.9 M HCl for 30 min at 22°C and rinsed with cold PBS. DNA probes were denatured for 5 min at 95°C and applied to coverslips which were sealed onto slides with rubber cement and incubated overnight at 37°C. Cells were then rinsed for 30 min with 2×SSC at 37°C, 2× SSC for 30 min at 22°C, 1×SSC for 30 min at 22°C and rinsed in PBS. Cells were mounted and counterstained as above.

Confocal microscopy and analysis

Cells were analyzed by confocal microscopy on a Leica SP2 or Leica SP5 AOBS system (Acousto-Optical Beam Splitter). Optical sections separated by 0.3 μm were collected, and only cells with signals from both alleles (typically over 95%) were analyzed using Leica software. Alleles were measured in 3-dimensions and pairing was defined as less than 1 μm distance. Alleles were defined as pericentromerically localized if the γ-satellite signal was overlapping or immediately juxtaposed. Alleles were defined as co-localized with γ-H2AX if the signals overlapped. Samples sizes were typically 200 cells minimum for association of alleles and upwards of 1000 cells for γ-H2AX co-localization. Statistical significances were calculated using χ^2 analysis as described47 in a pairwise analysis where each genotype and cell type was paired with the most biologically relevant differentiation stage or cell type. To avoid observer bias experiments were analyzed by more than one person.

Cell culture

Pro-B cell cultures were established using bone marrow cells enriched for $CD19^+$ cells by magnetic activated cell sorting (MACS) and cultured on OP9 stromal cells, in Iscove's modified Dulbecco's medium containing 2% serum, 0.03 % primatone RL (Mediatech), 4 mM glutamine, 50 μM β-mercaptoethanol, penicillin/streptomycin and 0.5 ng/ml IL-7 supernatant harvested from J558L IL-7 secreting cells. Murine embryonic fibroblasts were obtained from E13.5-15.5 embryos, head and visceral organs were removed, trypsinised and cultured for 4 days in Dulbecco's modified Eagle's medium with 10% serum, 1 mM glutamine, 50 μM β-mercaptoethanol and penicillin/streptomycin.

Analysis of *Igk* rearrangements in Abl pre-B cells

The generation and characterization of the *Atm*$^{-/-}$, *Artemis*$^{-/-}$, and *Artemis*$^{-/-}$*Atm*$^{-/-}$ Abelson pre-B cell lines were previously described29,32. The *Artemis*$^{-/-}$*p53*$^{-/-}$ Abelson pre-B cell lines were generated as described32 from *Artemis*$^{-/-}$ and *p53*$^{Flox/Flox}$ mice48 and then subject to Tat-Cre mediated deletion of *p53*. Induction and Southern blot analysis of *Igk* rearrangement in these cells also was previously described29,32. Nuclei of G1-arrested cells following STI571 treatment were isolated by hypotonic treatment, fixed in methanol:acetic acid (3:1 in volume), and subjected to interphase 2-color FISH using biotin- or digoxin-labeled BAC probes. After *Igk* break induction and release from STI571, cells were allowed to proliferate and re-enter the cell cycle, before Colcemid (Invitrogen) treatment and metaphase preparation according to standard protocols. The 5′ V_κ BAC RP24-243E11 and the 3′ C_κ BAC RP23-341D5 were purchased from Children's Hospital of Oakland Research Institute. Mouse whole chromosome paints were purchased from Applied Spectral Imaging (ASI). Images were captured using an Olympus BX61 microscope and a COOL-1300QS camera, and analyzed through Case Data Manager Version 5.5, installed and configured by ASI.

Analysis of allotypically marked *Igh* alleles in *Atm*$^{-/-}$ cells by flow cytometry

Lymphocytes from bone marrow, spleen and lymph nodes were stained with the following antibodies: FITC anti-mouse IgMa (BD Biosciences, clone DS-1), PE anti-mouse IgMb (Pharmingen, AF6-78), PE-Cy anti-B220 (Pharmingen, 552772), FITC mouse IgG1 isotype

control (Pharmingen, MOPC-31C), and PE mouse IgG1 isotype control (Pharmingen, MOPC-31C). Samples were RBC-depleted using NH_4Cl lysis buffer and stained in PBS containing 0.5% BSA. Live cells were gated on the basis of forward/side scatter and DAPI (Invitrogen, D1306) exclusion. Data was collected on an LSRII and analyzed with FlowJo.

Analysis of RSS breaks in sorted pro- and pre-B cells

Ligation Mediated PCR (LM-PCR) analysis of dsDNA breaks originating from the *Igh* locus was performed on sorted pro- and pre-B cell DNA samples as previously described 49,50.

Supplementary Material

Refer to Web version on PubMed Central for supplementary material.

Acknowledgements

This work was supported by a Wellcome Trust Project grant 085096 (J.A.S), New York University School of Medicine start-up funds (J.A.S), NIH grant R01 GM086852A (J.A.S), the Pew Scholars Program (C.H.B. and M.A.F), NIH grant R01 CA125195 (C.H.B.), NIH grant RO1 AI050737 (M.A.F), a Cancer Research Institute Predoctoral Emphasis Pathway in Tumor Immunology Training Grant awarded to the University of Pennsylvania School of Medicine (B.Y.), Boehringer Ingelheim (M.B.), an Austrian GEN-AU grant (M.B) and the National Institutes of Health and Howard Hughes Medical Institute (D.G.S.). We would like to thank members of the Skok lab for critical reading of this manuscript.

REFERENCES

1. Hesslein DG, Schatz DG. Factors and forces controlling V(D)J recombination. Adv Immunol. 2001; 78:169–232. [PubMed: 11432204]
2. Bassing CH, Swat W, Alt FW. The mechanism and regulation of chromosomal V(D)J recombination. Cell. 2002; 109(Suppl):S45–55. [PubMed: 11983152]
3. Hsu LY, et al. A conserved transcriptional enhancer regulates RAG gene expression in developing B cells. Immunity. 2003; 19:105–17. [PubMed: 12871643]
4. Gellert M. V(D)J recombination: RAG proteins, repair factors, and regulation. Annu Rev Biochem. 2002; 71:101–32. [PubMed: 12045092]
5. Roth DB. Restraining the V(D)J recombinase. Nat Rev Immunol. 2003; 3:656–66. [PubMed: 12974480]
6. Bassing CH, et al. Histone H2AX: a dosage-dependent suppressor of oncogenic translocations and tumors. Cell. 2003; 114:359–70. [PubMed: 12914700]
7. Celeste A, et al. Genomic instability in mice lacking histone H2AX. Science. 2002; 296:922–7. [PubMed: 11934988]
8. Chen HT, et al. Response to RAG-mediated VDJ cleavage by NBS1 and gamma-H2AX. Science. 2000; 290:1962–5. [PubMed: 11110662]
9. Morales JC, et al. Role for the BRCA1 C-terminal repeats (BRCT) protein 53BP1 in maintaining genomic stability. J Biol Chem. 2003; 278:14971–7. [PubMed: 12578828]
10. Perkins EJ, et al. Sensing of intermediates in V(D)J recombination by ATM. Genes Dev. 2002; 16:159–64. [PubMed: 11799059]
11. Fuxa M, et al. Pax5 induces V-to-DJ rearrangements and locus contraction of the immunoglobulin heavy-chain gene. Genes Dev. 2004; 18:411–22. [PubMed: 15004008]
12. Kosak ST, et al. Subnuclear compartmentalization of immunoglobulin loci during lymphocyte development. Science. 2002; 296:158–62. [PubMed: 11935030]
13. Roldan E, et al. Locus 'decontraction' and centromeric recruitment contribute to allelic exclusion of the immunoglobulin heavy-chain gene. Nat Immunol. 2005; 6:31–41. [PubMed: 15580273]

14. Sayegh C, Jhunjhunwala S, Riblet R, Murre C. Visualization of looping involving the immunoglobulin heavy-chain locus in developing B cells. Genes Dev. 2005; 19:322–7. [PubMed: 15687256]
15. Alt FW, et al. Ordered rearrangement of immunoglobulin heavy chain variable region segments. Embo J. 1984; 3:1209–19. [PubMed: 6086308]
16. Fitzsimmons SP, Bernstein RM, Max EE, Skok JA, Shapiro MA. Dynamic changes in accessibility, nuclear positioning, recombination, and transcription at the Igkappa locus. J Immunol. 2007; 179:5264–73. [PubMed: 17911612]
17. Goldmit M, et al. Epigenetic ontogeny of the Igk locus during B cell development. Nat Immunol. 2005; 6:198–203. [PubMed: 15619624]
18. Xu N, Tsai CL, Lee JT. Transient homologous chromosome pairing marks the onset of X inactivation. Science. 2006; 311:1149–52. [PubMed: 16424298]
19. Bacher CP, et al. Transient colocalization of X-inactivation centres accompanies the initiation of X inactivation. Nat Cell Biol. 2006; 8:293–9. [PubMed: 16434960]
20. Augui S, et al. Sensing X chromosome pairs before X inactivation via a novel X-pairing region of the Xic. Science. 2007; 318:1632–6. [PubMed: 18063799]
21. Jung D, Alt FW. Unraveling V(D)J recombination; insights into gene regulation. Cell. 2004; 116:299–311. [PubMed: 14744439]
22. Skok JA, et al. Reversible contraction by looping of the Tcra and Tcrb loci in rearranging thymocytes. Nat Immunol. 2007; 8:378–87. [PubMed: 17334367]
23. Hesslein DG, et al. Pax5 is required for recombination of transcribed, acetylated, 5′ IgH V gene segments. Genes Dev. 2003; 17:37–42. [PubMed: 12514097]
24. Nutt SL, Urbanek P, Rolink A, Busslinger M. Essential functions of Pax5 (BSAP) in pro-B cell development: difference between fetal and adult B lymphopoiesis and reduced V-to-DJ recombination at the IgH locus. Genes Dev. 1997; 11:476–91. [PubMed: 9042861]
25. Sonoda E, et al. B cell development under the condition of allelic inclusion. Immunity. 1997; 6:225–33. [PubMed: 9075923]
26. Fugmann SD, Villey IJ, Ptaszek LM, Schatz DG. Identification of two catalytic residues in RAG1 that define a single active site within the RAG1/RAG2 protein complex. Mol Cell. 2000; 5:97–107. [PubMed: 10678172]
27. Kim DR, Dai Y, Mundy CL, Yang W, Oettinger MA. Mutations of acidic residues in RAG1 define the active site of the V(D)J recombinase. Genes Dev. 1999; 13:3070–80. [PubMed: 10601033]
28. Landree MA, Wibbenmeyer JA, Roth DB. Mutational analysis of RAG1 and RAG2 identifies three catalytic amino acids in RAG1 critical for both cleavage steps of V(D)J recombination. Genes Dev. 1999; 13:3059–69. [PubMed: 10601032]
29. Bredemeyer AL, et al. DNA double-strand breaks activate a multi-functional genetic program in developing lymphocytes. Nature. 2008; 456:819–23. [PubMed: 18849970]
30. Yin B, Bassing CH. The sticky business of histone H2AX in V(D)J recombination, maintenance of genomic stability, and suppression of lymphoma. Immunol Res. 2008; 42:29–40. [PubMed: 18622584]
31. Callen E, et al. ATM prevents the persistence and propagation of chromosome breaks in lymphocytes. Cell. 2007; 130:63–75. [PubMed: 17599403]
32. Bredemeyer AL, et al. ATM stabilizes DNA double-strand-break complexes during V(D)J recombination. Nature. 2006; 442:466–70. [PubMed: 16799570]
33. Ma Y, Pannicke U, Schwarz K, Lieber MR. Hairpin opening and overhang processing by an Artemis/DNA-dependent protein kinase complex in nonhomologous end joining and V(D)J recombination. Cell. 2002; 108:781–94. [PubMed: 11955432]
34. Rooney S, et al. Artemis and p53 cooperate to suppress oncogenic N-myc amplification in progenitor B cells. Proc Natl Acad Sci U S A. 2004; 101:2410–5. [PubMed: 14983023]
35. Bertolino E, et al. Regulation of interleukin 7-dependent immunoglobulin heavy-chain variable gene rearrangements by transcription factor STAT5. Nat Immunol. 2005; 6:836–43. [PubMed: 16025120]

36. Chowdhury D, Sen R. Mechanisms for feedback inhibition of the immunoglobulin heavy chain locus. Curr Opin Immunol. 2004; 16:235–40. [PubMed: 15023418]
37. Joliot V, Cormier F, Medyouf H, Alcalde H, Ghysdael J. Constitutive STAT5 activation specifically cooperates with the loss of p53 function in B-cell lymphomagenesis. Oncogene. 2006; 25:4573–84. [PubMed: 16532027]
38. Goetz CA, Harmon IR, O'Neil JJ, Burchill MA, Farrar MA. STAT5 activation underlies IL7 receptor-dependent B cell development. J Immunol. 2004; 172:4770–8. [PubMed: 15067053]
39. Hewitt SL, et al. Association between the Igk and Igh immunoglobulin loci mediated by the 3′ Igk enhancer induces 'decontraction' of the Igh locus in pre-B cells. Nat Immunol. 2008; 9:396–404. [PubMed: 18297074]
40. Will WM, et al. Attenuation of IL-7 receptor signaling is not required for allelic exclusion. J Immunol. 2006; 176:3350–5. [PubMed: 16517702]
41. Li F, Eckhardt LA. A role for the IgH intronic enhancer E mu in enforcing allelic exclusion. J Exp Med. 2009; 206:153–67. [PubMed: 19114667]
42. Mombaerts P, et al. RAG-1-deficient mice have no mature B and T lymphocytes. Cell. 1992; 68:869–77. [PubMed: 1547488]
43. Shinkai Y, et al. RAG-2-deficient mice lack mature lymphocytes owing to inability to initiate V(D)J rearrangement. Cell. 1992; 68:855–67. [PubMed: 1547487]
44. Yu W, et al. Coordinate regulation of RAG1 and RAG2 by cell type-specific DNA elements 5′ of RAG2. Science. 1999; 285:1080–4. [PubMed: 10446057]
45. Barlow C, et al. Atm-deficient mice: a paradigm of ataxia telangiectasia. Cell. 1996; 86:159–71. [PubMed: 8689683]
46. Skok JA, et al. Nonequivalent nuclear location of immunoglobulin alleles in B lymphocytes. Nat Immunol. 2001; 2:848–54. [PubMed: 11526401]
47. Campbell, R. Statistics for Biologists. Cambridge University Press; 1989.
48. Jonkers J, et al. Synergistic tumor suppressor activity of BRCA2 and p53 in a conditional mouse model for breast cancer. Nat Genet. 2001; 29:418–25. [PubMed: 11694875]
49. Stanhope-Baker P, Hudson KM, Shaffer AL, Constantinescu A, Schlissel MS. Cell type-specific chromatin structure determines the targeting of V(D)J recombinase activity in vitro. Cell. 1996; 85:887–97. [PubMed: 8681383]
50. Liang HE, et al. The "dispensable" portion of RAG2 is necessary for efficient V-to-DJ rearrangement during B and T cell development. Immunity. 2002; 17:639–51. [PubMed: 12433370]

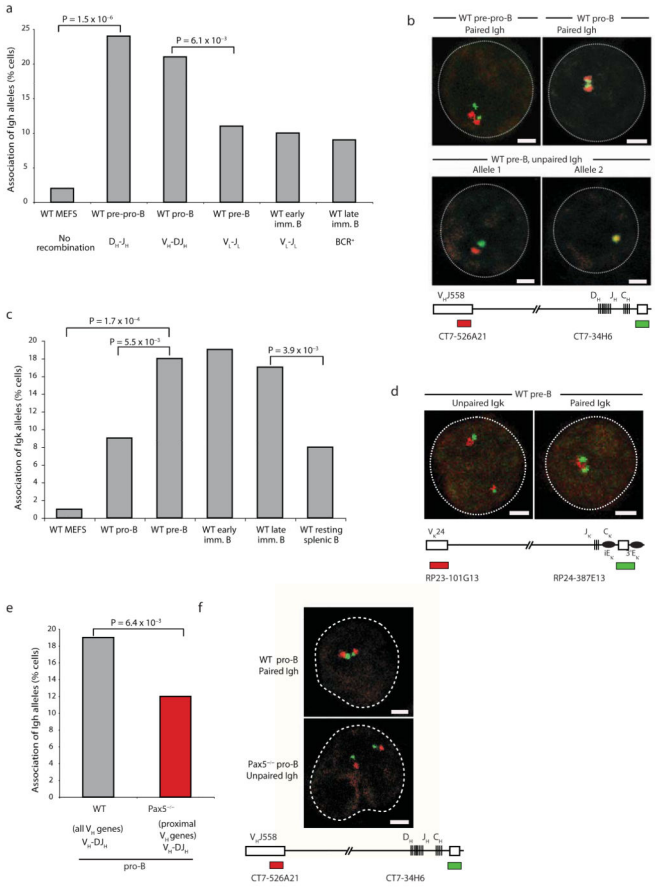

Figure 1.

Homologous pairing of *Igh* and *Igk* alleles occurs during recombination.

(**a**) Graph indicating the frequency of inter-allelic *Igh* pairing. 3-D DNA FISH analysis was carried out on *ex vivo* sorted cells of the indicated lineage and developmental stage. Pre-pro-B cells were sorted as lineage marker negative (Lin^-), $B220^+$, $CD19^-$, $cKit^+$, $CD25^-$, IgM^-. Pro-B cells were sorted as $CD19^+$, $cKit^+$, $CD25^-$, IgM^-, pre-B cells as $cKit^-$, $CD19^+$, $CD25^+$, IgM^-, early immature B cells as $CD19^+$, IgM^{lo}, IgD^- and late immature B cells as $CD19^+$, IgM^{hi}, IgD^-. (Supplementary Fig.1 and Methods online). Murine embryonic fibroblasts (MEFs) were obtained from E13.5-15.5 embryos and cultured for four days *in vitro*. DNA probes were generated from two bacterial artificial chromosomes, BACs CT7-526A21 (red signal) and CT7-34H6 (green signal), which map to the distal V_H gene region located at the 5′ end of the *Igh* locus and the 3′ constant (C_H) region, respectively. Pairing was determined by measuring the distance separating the two alleles. A cut-off separation of 1μm was used to define pairing. Data are representative of more than three independent experiments. The rearrangement status of the cells analyzed is indicated below each bar of the graph. Selected statistical significances according to the χ^2 test are shown between biologically relevant pairs. See Supplementary Table 1 for complete statistical results. (**b**) Confocal sections representative of paired and separated *Igh* alleles at the indicated stage of development. Decontracted *Igh* alleles are shown in pre-pro-B cells and contracted *Igh* alleles are shown in pro-B cells. A schematic representation of the position of probes used for detecting the

different regions of *Igh* in the 3-D DNA FISH analyses is shown. (**c**) Graph indicating the frequency of inter-allelic *Igk* pairing. 3-D DNA FISH analysis was carried out on *ex vivo* sorted cells of the indicated lineage and developmental stage. DNA probes used were generated from two bacterial artificial chromosomes, RP23-101G13 (red signal) and RP24-387E13 (green signal), which map to the distal $V_{\kappa}24$ gene region located at the 5′ end of the *Igk* locus and the 3′ constant (C_{κ}) region, respectively. (**d**) Confocal sections representative of paired and separated *Igk* alleles at the indicated stage of development. A schematic representation of the position of probes used for detecting the different regions of *Igk* in the 3-D DNA FISH analyses is shown. (**e**) Graph showing the frequency of inter-allelic *Igh* pairing in wild-type and *Pax5*$^{-/-}$ cultured pro B cells. The rearrangement status of the cells analyzed is indicated below the appropriate bar of the graph. (**f**) Confocal sections representative of paired contracted *Igh* alleles in wild-type pro-B cells and separated decontracted alleles in *Pax5*$^{-/-}$ pro-B cells. For all graphs selected statistical results are shown, see Supplementary Tables 1 and 2 online for complete statistical results. All data are representative of more than three independent experiments.

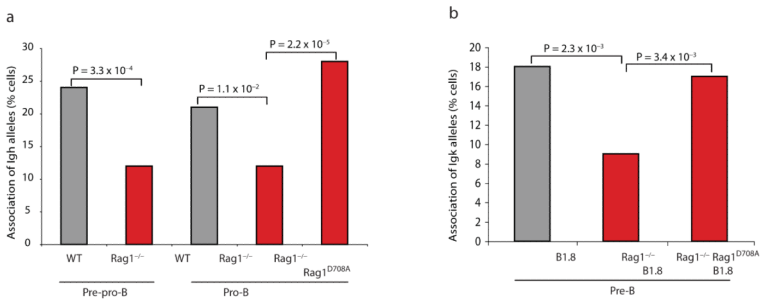

Figure 2.

RAG1 contributes to homologous pairing of *Igh* and *Igk* alleles.

(**a**) Graph indicating the frequency of inter-allelic *Igh* pairing in wild-type, *Rag1*$^{-/-}$ and in *Rag1*$^{-/-}$ pro-B cells containing the *Rag1* transgene with the active site mutation D708A. DNA FISH experiments were carried out as described for Fig. 1. (**b**) Graph indicating the frequency of inter-allelic *Igk* pairing in B1.8, B1.8 *Rag1*$^{-/-}$ and in B1.8 *Rag1*$^{-/-}$ pre-B cells containing the *Rag1* transgene with the active site mutation D708A. Selected statistical results are shown. See Supplementary Tables 1 and 2 for complete statistical results. Data are representative of at least three independent experiments.

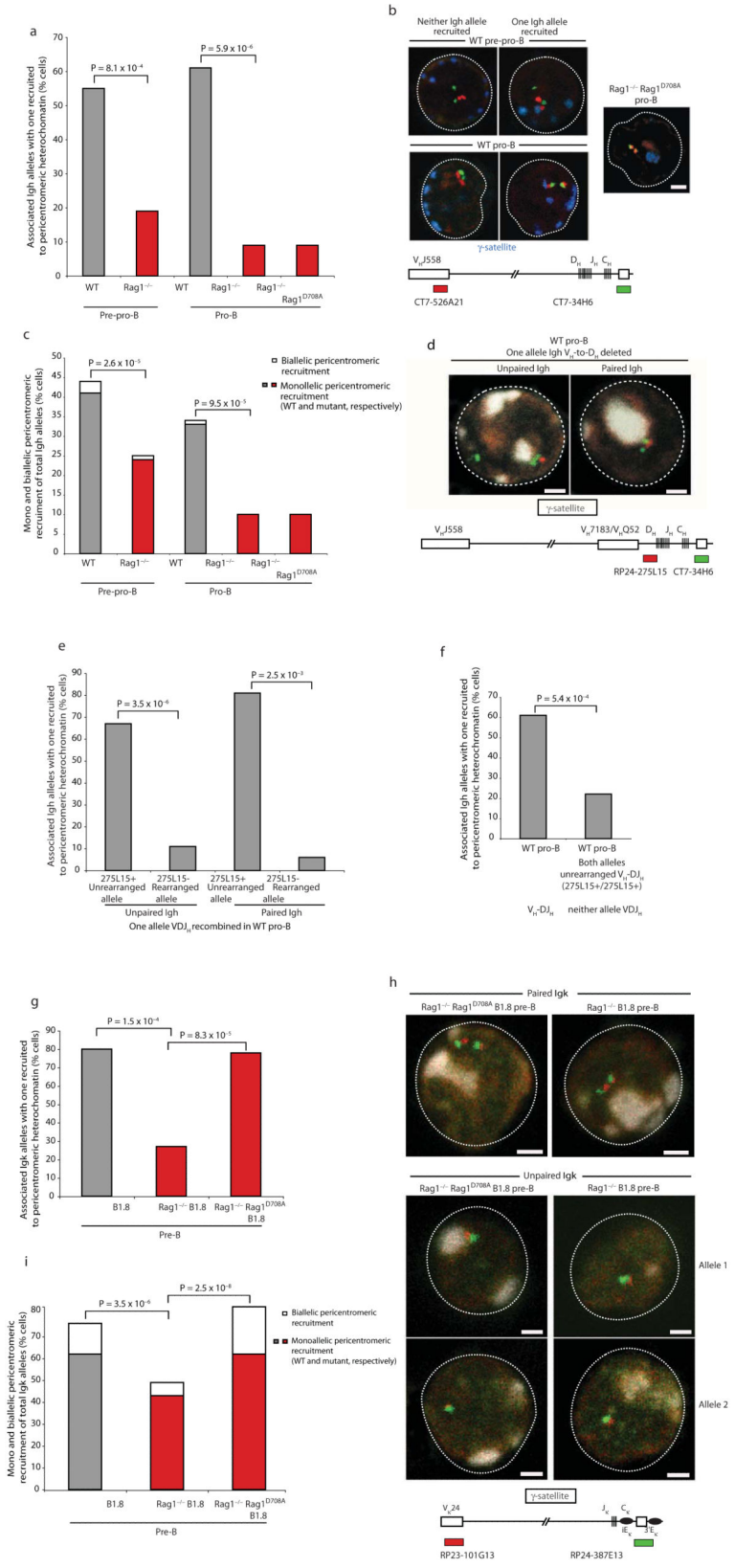

Figure 3.

RAG1 differentially marks paired *Ig* alleles as defined by their location within euchromatic and heterochromatic regions of the nucleus.

(**a**) Graph showing the frequency with which paired *Igh* alleles are positioned at pericentromeric heterochromatin in wild-type and *Rag1*$^{-/-}$ pre-pro-B and pro-B cells in addition to *Rag1*$^{-/-}$ pro-B cells containing a *Rag1-D708A* transgene. Alleles that are not located at pericentromeric heterochromatin are positioned within euchromatic regions of the nucleus. 3-D DNA FISH analysis was carried out on *ex vivo* sorted cells of the indicated lineage and developmental stage as described for Fig.1. DNA probes used were CT7-526A21 (red signal) and CT7-34H6 (green signal), which map to the distal V_H gene region located at the 5′ end of the *Igh* locus and the 3′ constant (C_H) region, respectively. A γ-satellite probe was used to detect pericentromeric heterochromatin. (**b**) Left panels — confocal sections representative of wild-type pre-pro-B and pro-B cells in which paired *Igh* alleles are equivalently located in euchromatin or differentially marked with one allele juxtaposed at pericentromeric heterochromatin. Right panel — confocal section representative of paired *Igh* alleles relative to pericentromeric heterochromatin in *Rag1*$^{-/-}$ pro-B cells containing the *Rag1-D708A* transgene. A schematic representation of the position of probes used for detecting the different regions of *Igh* in the 3-D DNA FISH analyses is shown. A γ-satellite probe was used to detect pericentromeric heterochromatin (blue signal). (**c**) Mono and biallelic pericentromeric recruitment of all *Igh* alleles in wild-type, *Rag1*$^{-/-}$ and *Rag1*$^{-/-}$ pre-pro-B and pro-B cells and pro-B cells containing the *Rag1-D708A* transgene. (**d**) Confocal sections representative of unpaired and paired *Igh* alleles relative to pericentromeric heterochromatin in cells with one rearranged VDJ_H allele. Unrearranged alleles are indicated by the presence of a BAC signal for the V_H to D_H region RP24-275L15 (red signal), alongside a C_H CT7-34H6 probe (green signal). A schematic representation of the position of probes used for detecting the different regions of *Igh* in the 3-D DNA FISH analyses is shown. A γ-satellite probe was used to detect pericentromeric heterochromatin (white signal). Rearranged alleles are indicated by the presence of a single BAC signal, CT7-34H6 (green signal). (**e**) Graph showing the frequency with which rearranged or unrearranged *Igh* alleles are positioned at pericentromeric heterochromatin in cells with one V_H-to-DJ_H rearranged allele. The analysis was performed on cells with unpaired or paired alleles, as indicated. The rearrangement status of the cells analyzed is indicated below the graph. (**f**) Graph showing the frequency with which paired *Igh* alleles are positioned at pericentromeric heterochromatin in wild-type pro-B cells irrespective of rearrangement status and in comparison to paired unrearranged alleles containing the intergenic V_H-D_H region of the *Igh* locus (as judged by the presence of both BAC RP24-275L15 signals). Probes used are described in c and the rearrangement status of the cells analyzed is indicated below the appropriate bar of the graph. For all data, selected statistical results are shown. See Supplementary Tables 4, 5 and 6 for complete statistical results. All data are representative of three independent experiments.

Figure 3 part 2 (**g**) Graph showing the frequency with which paired *Igk* alleles are positioned at pericentromeric heterochromatin in B1.8, B1.8 *Rag1*$^{-/-}$ and B1.8 *Rag1*$^{-/-}$ pre-B cells containing the *Rag1* transgene with the active site mutation D708A. Probes used were RP23-101G13 (red signal) and RP24-387E13 (green signal), which map to the distal $V_κ24$ gene region located at the 5′ end of the *Igk* locus and the and the 3′ constant ($C_κ$)

region, respectively. (**h**) Upper panels — Confocal sections representative of differentially marked paired alleles in B1.8 and B1.8 *Rag1*$^{-/-}$ pre-B cells containing the *Rag1* transgene with the active site mutation D708A and paired alleles located equivalently in euchromatic regions in *Rag1*$^{-/-}$ pre-B cells. A γ-satellite probe (white signal) was used to detect pericentromeric heterochromatin. Lower panels — Confocal sections showing the position of unpaired *Igk* alleles relative to pericentromeric heterochromatin in B1.8 *Rag1*$^{-/-}$ and B1.8 *Rag1*$^{-/-}$ pre-B cells containing the *Rag1* transgene with the active site mutation D708A. (**i**). Mono and biallelic pericentromeric recruitment of all *Igk* alleles in B1.8, B1.8 *Rag1*$^{-/-}$ and B1.8 *Rag1*$^{-/-}$ pre-B cells containing the *Rag1* transgene with the active site mutation D708A. For all graphs selected statistical results are shown. See Supplementary Tables 7 and 8 for complete statistical results. Results are representative of three independent experiments.

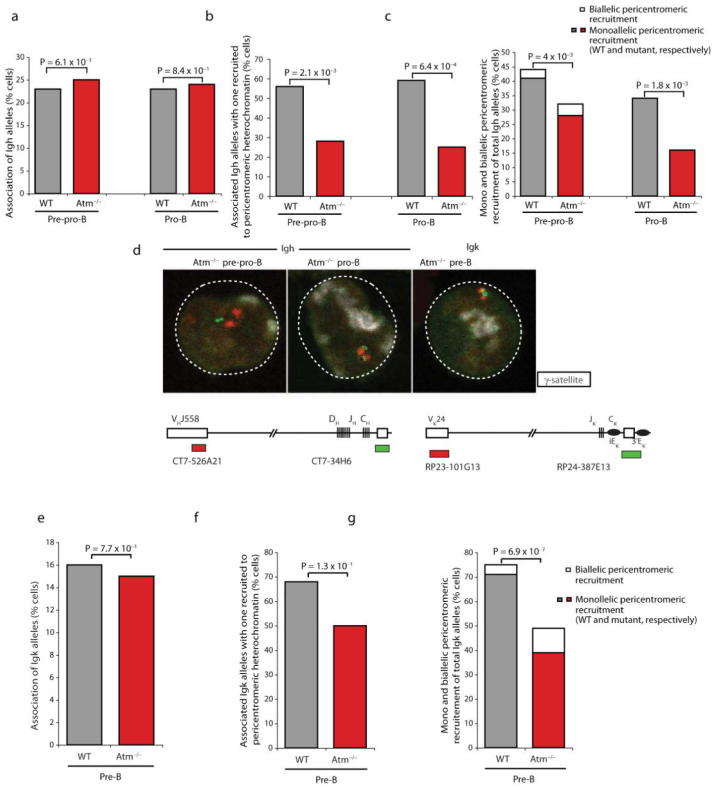

Figure 4.

ATM directs repositioning of one *Ig* allele to pericentromeric heterochromatin. (**a**) Graph indicating the frequency of interallelic *Igh* pairing in wild-type and *Atm*$^{-/-}$ pre-pro-B and pro-B cells. The developmental profile of *Atm*$^{-/-}$ compared to wild-type sorted bone marrow primary B lymphocytes is described in Supplementary Fig. 2 (online). (**b**) Graph showing the frequency with which paired *Igh* alleles are positioned at pericentromeric heterochromatin in wild-type and *Atm*$^{-/-}$ pre-pro-B and pro-B cells. (**c**) Mono and biallelic pericentromeric recruitment of total *Igh* alleles in wild-type and *Atm*$^{-/-}$ pre-pro-B and pro-B cells. (**d**) Confocal sections showing the position of undifferentially marked paired *Igh* and *Igk* alleles at the indicated stages of development. Probes used in these experiments are indicated. (**e**) Graph indicating the frequency of interallelic *Igk* pairing in wild-type and *Atm*$^{-/-}$ pre-B cells. (**f**) Graph showing the frequency with which paired *Igk* alleles are positioned at pericentromeric heterochromatin in wild-type and *Atm*$^{-/-}$ pre-B cells. (**g**) Mono and biallelic pericentromeric recruitment of *Igk* in wild-type and *Atm*$^{-/-}$ pre-B cells. For all graphs selected statistical results are shown. See Supplementary Tables 1, 2, 5, 6, 7 and 8 for complete statistical results. All results shown are representative of three independent experiments.

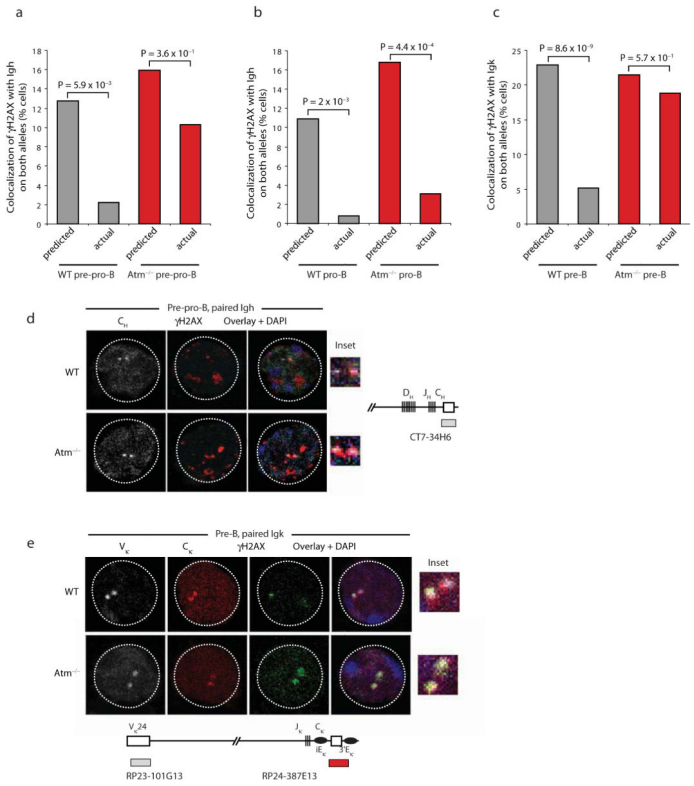

Figure 5.

ATM prevents bi-allelic RAG-mediated cleavage during *Ig* V(D)J rearrangement.

(**a**) Graph showing the predicted and actual percentages of cells with biallelic colocalization of γ-H2AX on *Igh* in wild-type and *Atm*$^{-/-}$ pre-pro-B cells. This percentage is calculated based on the total percentage of pre-pro-B cells with mono or biallelic colocalization of γ-H2AX on *Igh* alleles. (**b**) Graph showing the predicted and actual percentages of cells with biallelic colocalization of γ-H2AX on *Igh* in wild-type and *Atm*$^{-/-}$ pro-B cells. This percentage is calculated based on the total percentage of pro-B cells with mono or biallelic colocalization of γ-H2AX on *Igh* alleles. (**c**) Graph showing the predicted and actual percentages of cells with biallelic colocalization of γ-H2AX on *Igk* in wild-type and *Atm*$^{-/-}$ pre-B cells. This percentage is calculated based on the total percentage of pre-B cells with mono or biallelic colocalization of γ-H2AX on *Igk* alleles. (**d**) Individual and merged confocal microscopy sections indicate the localization of γ-H2AX foci on *Igh* alleles in sorted wild-type and *Atm*$^{-/-}$ pre-pro-B cells. Immunofluorescence staining indicates γ-H2AX foci (red). The DNA probe CT7-526A21 (white signal) indicates the position of the 3′ constant (C_H) region. Representative cells show paired *Igh* alleles with γ-H2AX localized mono-allelically in wild-type pre-pro-B cells and bi-allelically in *Atm*$^{-/-}$ pre-pro-B cells. Right hand panels show enlarged *Igh* alleles. (**e**) Individual and merged confocal microscopy sections indicate the localization of γ-H2AX foci on *Igk* alleles in sorted wild-type and *Atm*$^{-/-}$ pre-B cells. Immunofluorescence staining indicates γ-H2AX foci (green). DNA probes RP23-101G13 (white signal) and RP24-387E13 (red signal) indicate the position of the distal V_K gene region located at the 5′ end of the *Igk* locus and the 3′ constant (C_K) region, respectively. Representative cells show paired *Igk* alleles with γ-H2AX localized

mono-allelically in wild-type pre-B cells and bi-allelically in *Atm*$^{-/-}$ pre-B cells. Right hand panels show enlarged *Igk* alleles. For all graphs selected statistical results are shown. See Supplementary Tables 9 and 10 for complete statistical analysis. All results shown are representative of three independent experiments.

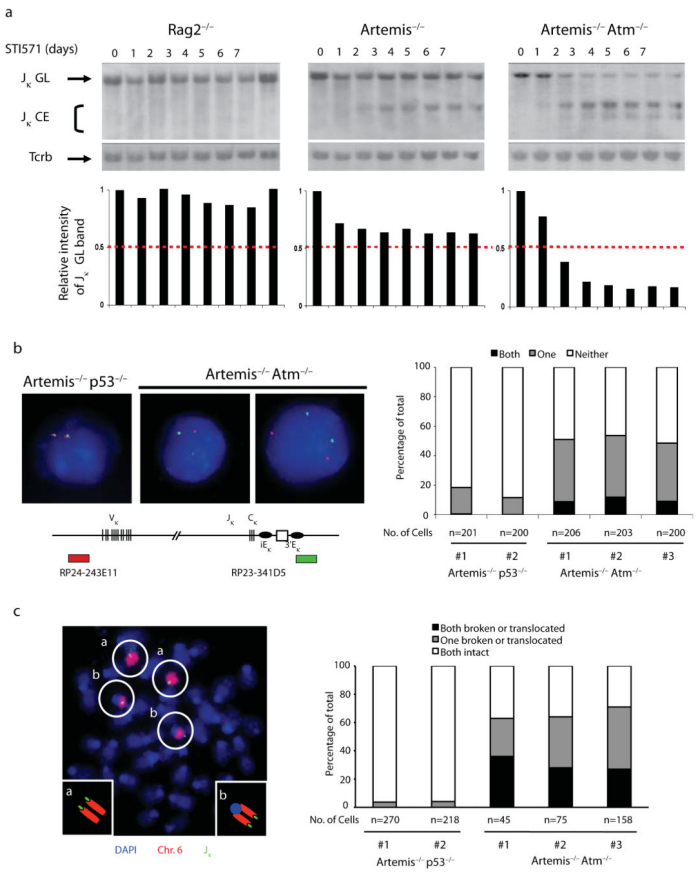

Figure 6.

ATM prevents bi-allelic *Igk* chromosome breaks and translocations.

(**a**) Southern blot analysis of the *Igk* locus was performed on *Bam*HI-digested genomic DNA isolated from *Rag2*$^{-/-}$, *Artemis*$^{-/-}$, and *Artemis*$^{-/-}$*Atm*$^{-/-}$ Abelson pre-B cell lines treated with STI571 for the indicated number of days. The top panel depicts blots hybridized with a 3′J_κ probe. Bands corresponding to germline *Igk* (J_κ GL) and un-repaired J_κ coding ends (J_κ CE) are indicated. The same blots were stripped and re-hybridized with a *Tcrb* locus probe to account for DNA amounts. The intensity of the germline J_κ band was normalized to that of the *Tcrb* band to represent RAG-mediated *Igk* cutting within each population of cells. (**b**) Quantification of RAG-induced *Igk* genomic instability during V(D)J recombination in pre-B cell lines. Left, representative light microscopy images of two-color FISH analysis conducted on G1 phase nuclei of STI571 treated *Artemis*$^{-/-}$*p53*$^{-/-}$ and *Artemis*$^{-/-}$*Atm*$^{-/-}$ pre-B cells using a 5′V_κ BAC (red signal) and 3′C_κ BAC (green signal) and DAPI to visualize DNA. Right, graph showing the number and percentage of *Artemis*$^{-/-}$*p53*$^{-/-}$ and *Artemis*$^{-/-}$*Atm*$^{-/-}$ pre-B cells with coincident (C) and non-coincident (NC) hybridization of the 5′V_κ and 3′C_κ signals. The percentages of cells with separated signals on both alleles are statistically different ($P = 0.005$) between *Artemis*$^{-/-}$*p53*$^{-/-}$ and *Artemis*$^{-/-}$*Atm*$^{-/-}$ pre-B cells. (**c**) Quantification of RAG-induced *Igk* chromosome breaks or translocations during V(D)J recombination in pre-B cell lines. Left, representative light microscopy images of whole chromosome 6 (red) paints and FISH analysis using the 5′V_κ and 3′C_κ BACs (green signals) and DAPI (blue) to visualize DNA on metaphases prepared from STI571-treated and

released *Artemis*$^{-/-}$*p53*$^{-/-}$ and *Artemis*$^{-/-}$ *Atm*$^{-/-}$ pre-B cells. Right, graph showing the percentage of STI571 treated and released pre-B cell lines with *Igk* chromosome breaks or translocations on one or both copies of chromosome 6. All data shown are representative of at least three independent experiments.

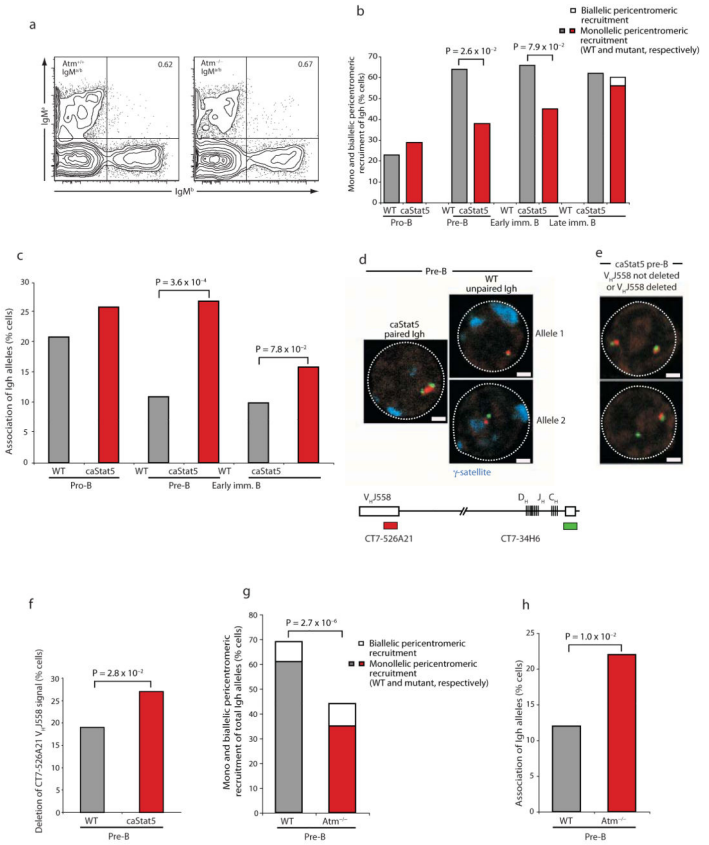

Figure 7.

Igh pairing can occur beyond the pro-B cell stage if locus accessibility is maintained. (**a**) Flow cytometric analysis of bone marrow cells from wild-type and *Atm*$^{-/-}$ mice heterozygous for two allotypically marked *Igh* alleles. (**b**) Graph showing mono- and biallelic recruitment of *Igh* at different developmental stages in *ex vivo* sorted wild-type (grey bars) and *caStat5* (red bars) B lymphocytes. 3-D DNA FISH was carried out as described for Fig. 1. (**c**) Graph showing frequency of association of *Igh* alleles in sorted wild-type and *caStat5* pre-B and immature B cells. (**d**) Confocal sections showing tightly paired *Igh* alleles in a *caStat5* pre-B cell. Representative confocal sections indicate the position and conformation of non-associating *Igh* alleles in a wild-type pre-B cell. DNA probes used in the FISH experiments are as indicated. (**e**) Confocal sections showing cells with (right) and without (left) deletion of one CT7-526A21 V_HJ558 signal. Probes used in this experiment are indicated in d. (**f**) The frequency of deletion of the CT7-526A21 V_HJ558 signal in wild-type and *caStat5* pre-B cells is shown in the graph. (**g**) Graph showing mono- and biallelic recruitment of *Igh* at in *ex vivo* sorted wild-type (grey bars) and *Atm*$^{-/-}$ (red bars) pre-B cells. (**h**) Graph showing frequency of association of *Igh* alleles in sorted wild-type (grey bars) and *Atm*$^{-/-}$ (red bars) pre-B cells. For all graphs, selected statistical results are shown. See Supplementary Table 6 and 8 for complete statistical results. All results shown are representative of three independent experiments.